

Experimental study on fire performance of axially-restrained NSC and HSC columns

Bo Wu[†] and Yi-Hai Li[‡]

State Key Laboratory of Subtropical Building Science, South China University of Technology, Guangzhou, 510640, China

(Received February 16, 2009, Accepted June 17, 2009)

Abstract. This paper describes fire performance of eight axially restrained reinforced concrete (RC) columns under a combination of two different load ratios and two different axial restraint ratios. The eight RC columns were all concentrically loaded and subjected to ISO834 standard fire on all sides. Axial restraints were imposed at the top of the columns to simulate the restraining effect of the rest of the whole frame. The axial restraint was effective when the column was expanding as well as contracting. As the results of the experiments have shown, the stiffness of the axial restraint and load level play an important role in the fire behaviors of both HSC and NSC columns. It is found that (a) the maximum deformations during expanding phase were influenced mostly by load ratio and hardly by axial restraint ratio, (b) For a given load ratio, axial restraint ratio had a great impact on the development of axial deformation during contraction phase beyond the initial equilibrium state, (c) increasing the axial restraint increased the value of restraint force generated in both the NSC and HSC columns, and (d) the development of column axial force during the contracting and cooling phase followed nearly parallel trend for columns under the same load ratio.

Keywords: high-strength concrete; column; fire performance; axial restraint; cooling phase.

1. Introduction

In recent years, reinforced concrete (RC) columns with high-strength concrete (HSC) have been gaining popularity in the engineering industry for their high performing material compared to normal-strength concrete (NSC). In general, concrete columns exhibit satisfying fire performance under fire conditions. However, studies have shown that HSC is more susceptible to spalling because of its low permeability, which will in return reduce the fire resistance remarkably. The growing use of HSC has caused a debate concerning the fire safety of this type of concrete. At present, the methods in codes and standards for the fire safety design of RC columns are based on traditional standard fire tests on isolated members. However, columns acting as part of a frame exhibit different behavior from that of isolated ones in fire, because of the considerable restraint and continuity provided by abutting structure. Axial restraint, in particular, may accelerate the columns failure due to the additional axial forces generated in columns during expanding phase.

[†] Professor, Ph.D., Engineering Science, Corresponding author, E-mail: bowu@scut.edu.cn

[‡] Ph.D. Student, E-mail: yihai.li@mail.scut.edu.cn

In the past decade, research has been concentrated on the behavior of restrained steel and composite columns in fire (Ali and O'Connor 2001, Ali *et al.* 1998, Cabrita Neves 1995, Cabrita Neves *et al.* 2002, Huang and Tan 2004, Huang *et al.* 2006, 2007, Rodrigues *et al.* 2000, Tan *et al.* (2007, Valente and Neves 1999, Wang 1997, 1999, Wang and Davies 2003a, 2003b, 2003c), in which the stiffness of the restraint was considered unchanged during the fire test. However, the same level of development has not taken place for reinforced concrete columns. Ali *et al.* (2004) have reported a research on 93 half-scale restrained high and normal strength concrete columns subjected to fire, with special focus on concrete spalling. Benmarce *et al.* (2005) have conducted a study of 12 restrained high strength concrete columns under fire. In both of the previous two tests, axial restraint was imposed to the column by employing specially designed rubber springs, which was effective only when the column was expanding. Because of the test setup, the main disadvantage of the two tests is that the test stopped when the column displacement and axial force went back to initial equilibrium state, i.e., zero displacement before heating. However, in reality, columns in a frame should be able to undergo further contraction with the aid of restraint from surrounding structure. Moreover, natural fires including cooling phase are common in a real fire. Columns are likely to be restrained by adjacent members because of further deterioration of materials during cooling phase. None of these has been appropriately addressed in the test before.

To the authors' best knowledge, there has been no test carried out to follow the entire expanding and contracting phase including cooling phase. The current research project is funded to investigate experimentally the full behaviors of restrained HSC and NSC column during fire. The paper outlines the experimental program and presents the experimental results of fire performance of eight axially restrained RC columns (four of HSC and four of NSC).

2. Experimental program

2.1 Test specimens

Two main factors considered in the experimental research were load ratio and axial restraint ratio, as listed in Table 1; in which k_c , k_l , β and α denote axial stiffness of column, axial restraint stiffness, axial restraint ratio and load ratio, respectively. All columns have a nominal height of 2340 mm and only the central portion of 1650 mm was exposed to fire on all sides. Each column was reinforced with 4 longitudinal rebars of HRB400 with a diameter of 18 mm. For all tested

Table 1 Summary of specimen parameters

Type of concrete	Column No.	α	k_c (MN/m)	k_l (MN/m)	β
NSC	RCN11	0.24	672.1	34.5	0.0513
	RCN12	0.25	672.1	51.9	0.0772
	RCN21	0.35	672.1	34.5	0.0513
	RCN22	0.35	672.1	51.9	0.0772
HSC	RCH11	0.24	775.1	34.5	0.0445
	RCH12	0.25	775.1	51.9	0.0670
	RCH21	0.33	775.1	34.5	0.0445
	RCH22	0.34	775.1	51.9	0.0670

columns, the steel ratio is 2.54%. Steel bars of HPB235 with a diameter of 8 mm were used for ties, which were spaced at 100 mm within the central portion. Closer tie spacing of 50 mm was used within the unheated part and near the column end. All lateral reinforcements were bent at 135°.

In order to ensure the connectivity and avoid local failure of concrete near the top and bottom ends of the specimens, the enlarged portions with dimensions of 400×400×325 mm and the 20 mm steel plate at both ends of the column were wrapped with ceramic fiber blanket. The mechanical properties of materials measured experimentally are summarized in Table 2 and specimen details are shown in Fig. 1.

Table 2 Material properties

Concrete type	f_c (MPa)	E_c (MPa)	Rebar	f_y (MPa)	E_s (MPa)
NSC	29.8	34400	Main bar (Grade II)	402.1	200000
HSC	57.0	40500	Tie (Grade I)	315.6	200000

Note: Values are average of the four samples. Elastic modulus is not measured and calculated according to EC2 (2004).

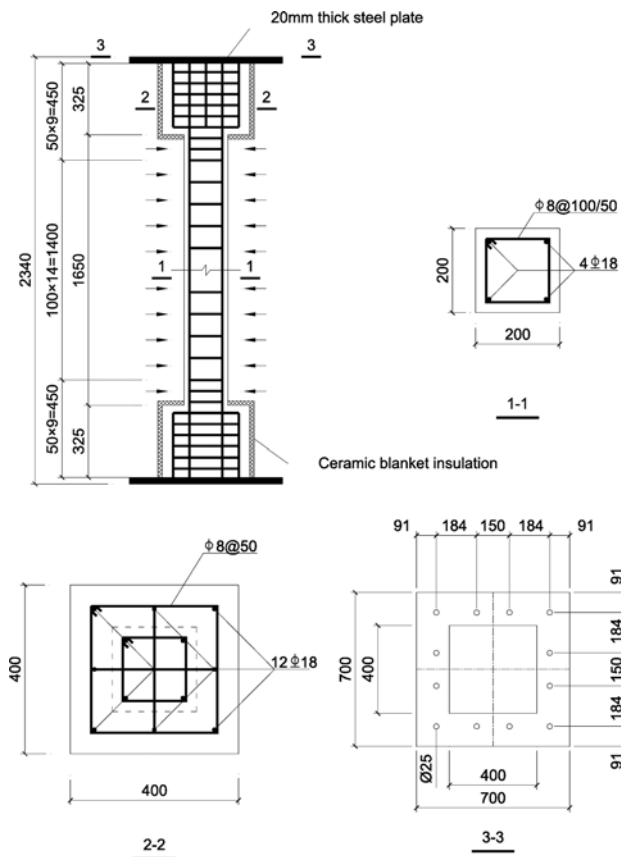


Fig. 1 Details of test specimens (Note: All dimensions are in mm)

2.2 Test setup and furnace construction

The tests were performed under transient heating state conditions, i.e., the column was loaded at room temperature and the load was kept constant during the fire exposure. Fig. 2 shows the test set-

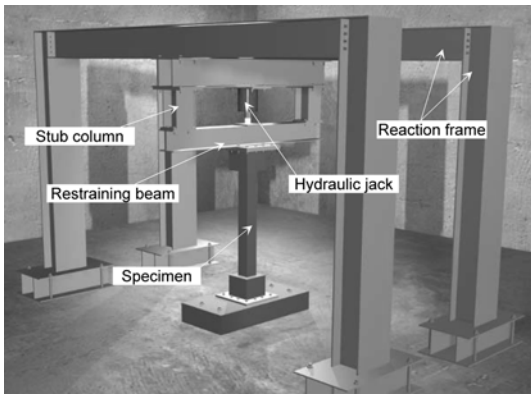


Fig. 2 Test setup

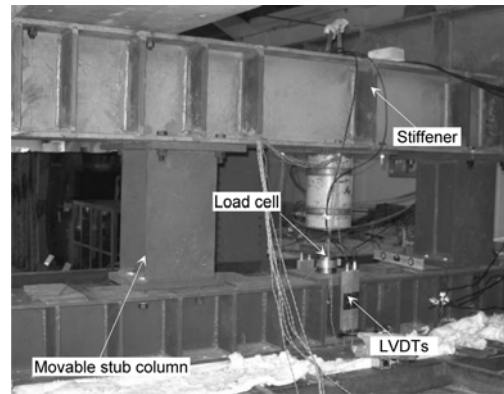


Fig. 3 Details of restraining beam

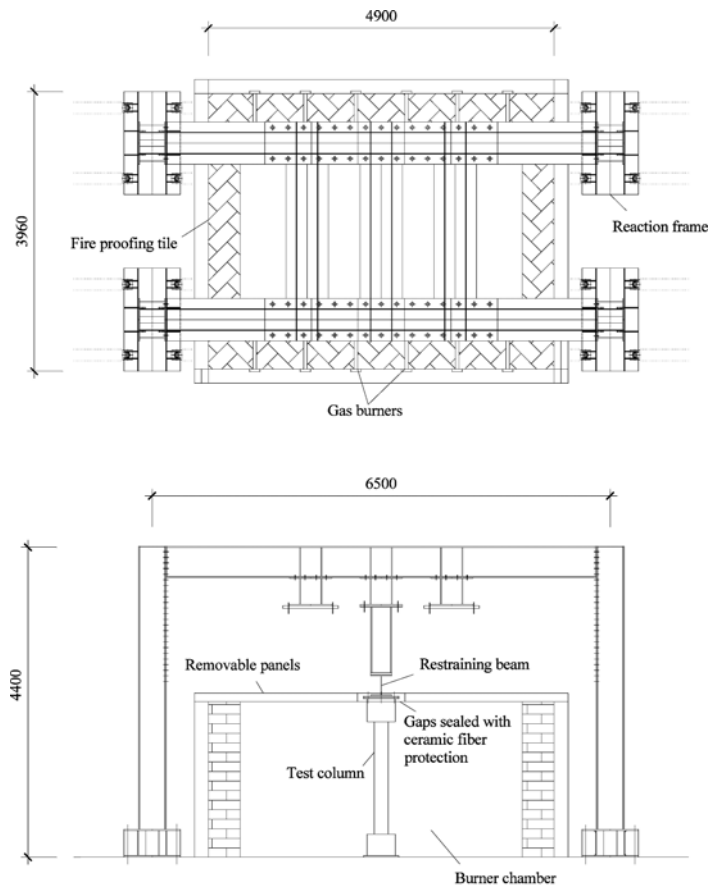


Fig. 4 Furnace construction and testing assembly (Note: All dimensions are in mm)

up (cf. Fig. 10). Each test assembly consisted of a RC column and a restraining beam (Fig. 3). The bottom end plate of the RC column was fixed to the ground base by 12 bolts to simulate fixed-end support. The column top steel plate was connected to the bottom flange of the restraining beam by bolts, which was restrained from rotation during the test. A reaction frame constructed outside the furnace and fixed to the ground, was used to apply the vertical loads. Ribbed stiffeners were welded to the reaction frame and the restraining beam to avoid any local failure. The reaction frame has a testing capacity of 1200 kN.

The tests were carried out in one of the three furnaces in the fire laboratory at South China University of Technology. Fig. 4 shows the furnace construction. The internal dimension of this furnace is 4×3×1.5 m. Two upper panels of the furnace are removable to facilitate assembly of the test specimens. Openings between the panels were filled with ceramic fibers and insulation boards, which ensured that the restraining beam remained unheated during the tests. The furnace consists of 24 gas burners, with firing and control equipment installed and connected to a computer. The gas burners are evenly and symmetrically distributed on the north and south sides of the furnace. Average temperature inside the furnace is recorded by 8 embedded thermocouples and automatically controlled by the computer to follow the standard ISO834 fire curve.

2.3 Loading facility and test measurements

The restraining beam and the column-to-beam connection were projected outside the furnace to facilitate the application of load. The vertical load was imposed on the top flange of the restraining beam by a hydraulic jack. Additional axial load generated during the expanding phase was carried by the restraining beam. During the contracting phase beyond the initial equilibrium state, the vertical load was gradually transferred to the restraining beam supported on the reaction frame. Different axial restraint stiffnesses were obtained by varying the length of the restraining beam (i.e., by moving the stub columns, see Fig. 3). The restraint stiffnesses of the axial restraining system were measured experimentally after the fabrication and reassembly several times. The repeatability is good and average values of the axial restraint stiffness are given in Table 1.

Four thermocouples were embedded within the mid-height cross section for each test specimen, as shown in Fig. 5. For each test assembly, two additional thermocouples, one attached to the bottom flange of the restraining beam and the other attached to the surface of the enlarged section, were used to check the influence of high temperature. All thermocouples were connected to the computer and temperatures were recorded automatically every one minute.

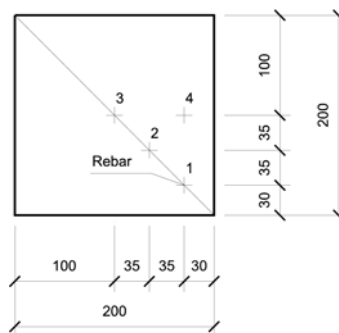


Fig. 5 Locations of thermocouples within cross section (Note: All dimensions are in mm)

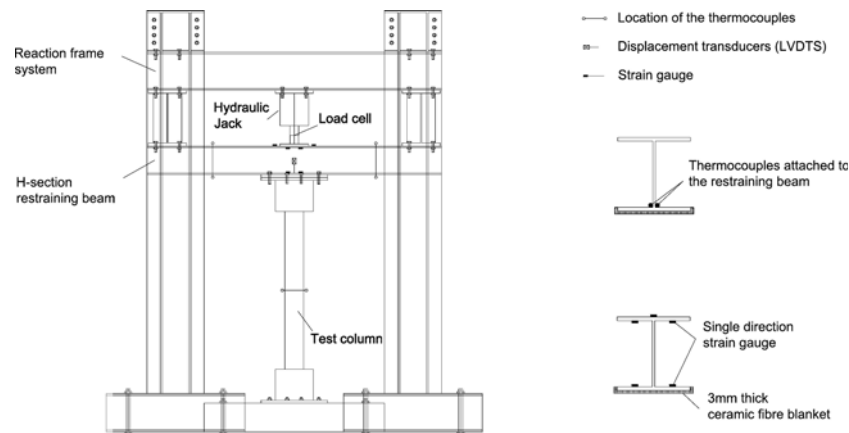


Fig. 6 Distribution of the thermocouples and strain gauges over the cross section

Axial deformations were measured using four linear variable displacement transducers (LVDTs) symmetrically located at the top end plate of column (Fig. 3). A load cell attached to the hydraulic jack was used to measure the applied load, which was kept constant during the test. No strain gauge could be placed on columns because of the high temperature during the fire attack. Thus, the axial force in a test column can not be obtained directly. In this way, a total number of six strain gauges were positioned on the restraining flange beam. For each test, the sum of force taken by the restraining beam and the applied load was then deemed to give the axial force in column. Fig. 6 shows the positions of the strain gauges.

3. Test procedure

Before the commencement of fire exposure, axial load was imposed on the top flange of the restraining beam, which had been connected to the column top steel plate but was not connected to the reaction frame. It ensured that the entire load was held by column. The procedures for setting up and performing a test on a restrained concrete column under transient heating state are outlined as follows:

- Setting up the specimen in the test rig and connecting the restraining beam to the column.
- Preloading (50% of the working load) and unloading the specimen twice to minimize the mechanical slacks in the test rig.
- Applying the working load to the top flange of the restraining beam and then holding it constant for 10 minutes to stabilize the deformation.
- Connecting the restraining beam to the reaction frame and securing the possible gaps until the strain gauges gave small readings, indicating proper contact.
- Positioning the LVDTs on the specimen and connecting LVDT wires to a data logger.
- Joining wires of the thermocouples and strain gauges to a computer system.
- Turning on the gas burners and heating up the column while maintaining the applied load.

Unless columns failed prematurely, the gas burners were switched off at around 120 min after the ignition in order to initiate a cooling phase. The test was finally terminated when the average temperature in the furnace fell back to around 300°C at about 180 min.

4. Experimental results and discussion

The test program consists of four fire tests on RC columns, with a combination of two kinds of axial restraint stiffness and two levels of loading for each type of concrete. The purpose of the research project is to study the behaviors of restrained concrete columns with different load ratios and restraint ratios under both expanding and contracting processes, including cooling phase. The results of measured temperature fields, axial displacements and axial forces are presented and discussed.

4.1 Visual observations-Spalling of specimens after fire test

Very little could be observed during the test because the columns were enclosed in the furnace. Several loud popping sounds were heard during the initial 10-15 min for test RCH12 and RCH22, which might be caused by concrete explosive spalling. Fig. 7 shows the pictures of the specimens

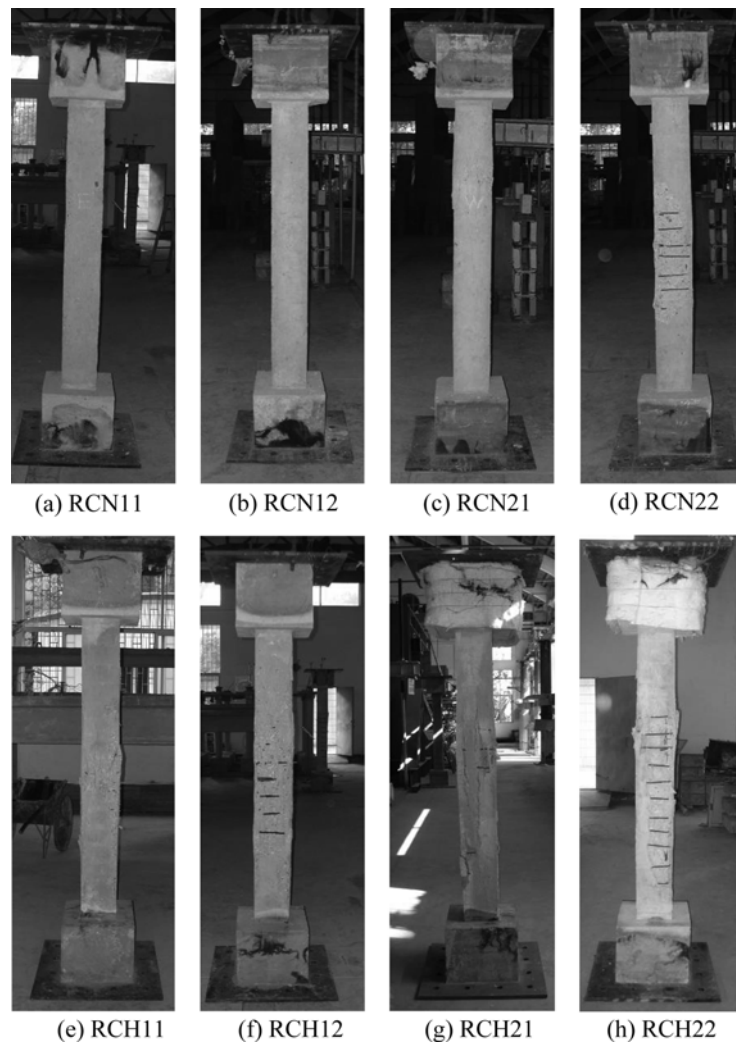


Fig. 7 Pictures of tested columns after cooling to room temperature: (a)-(d) NSC columns, (e)-(h) HSC columns

after test. There were mainly small vertical cracks on all sides of columns. None of the four NSC columns failed during the fire test, while three of the HSC columns (RCH11, RCH21 and RCH22) showed a very brittle type of failure. It can be seen that the concrete near the middle of column height was crushed for the three failed HSC columns, with very large visible vertical cracks. Spalling was observed for three columns (RCH12, RCH22 and RCN22), confirming the popping sounds accompanying spalling. The axial restraint ratio seems to have an effect on concrete spalling. The more axial restraint a specimen was imposed, the more likelihood that concrete spalling would happen.

Spalling of concrete during fire is complicated and therefore there is no unanimous agreement on when and to which extent spalling will take place. Some test data show that spalling is influenced by the stirrup configuration: spalling occurs only outside the reinforcement cage with ties bent at 135°, while it occurs throughout the cross section in a conventional pattern. As the experimental observations after fire have indicated, spalling of concrete occurred to the depth of the outer surface of longitudinal bars. This can be attributed to the modified tie configuration.

4.2 Temperature distribution

Fig. 8 shows the average recorded temperature curves of furnace atmosphere for the eight tests. The designed heating period of all tests is two hours, after which a cooling period is followed. As we can see for NSC columns, the ISO standard curve was followed quite well during the heating phase except for specimen RCN21 from 70 min to 90 min where a thermocouple gave an error reading. The furnace parameters were shifted to manual control at the beginning of the cooling phase to ensure a similar one-hour cooling path for all tests. As for HSC columns, three of the test specimens (RCH11, RCH21 and RCH22) suddenly failed before 120 min, thus no cooling phase was followed. Due to the malfunction of the computer controlling for the test specimen RCH12, the furnace temperature during the first 30 minutes was considerably higher than the corresponding temperature of ISO standard curve. The temperature was manually tuned to follow closely the ISO curve until 180 minutes, during which no failure was observed.

For HSC columns, explosive spalling altered the sectional temperature fields significantly for specimens RCH12 and RCH22. The side near which thermocouples 1 and 4 were located was

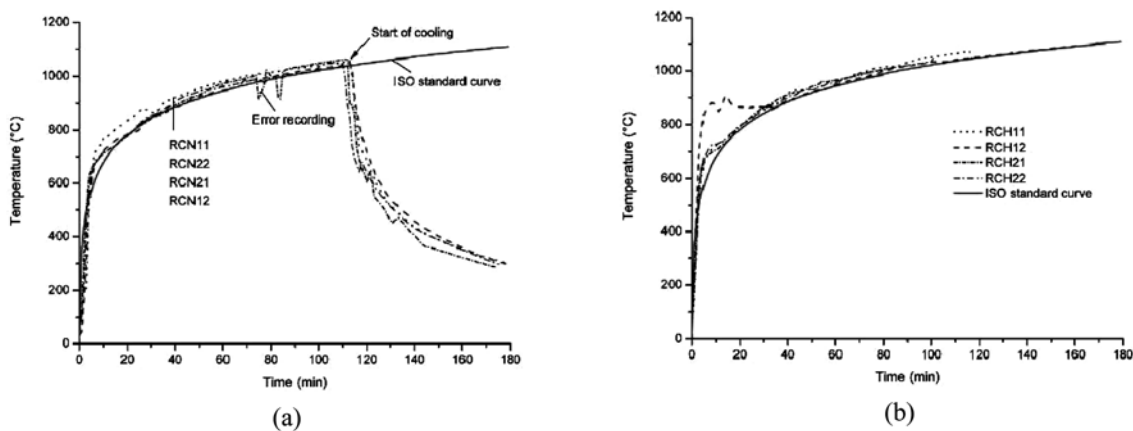


Fig. 8 Recorded average temperature-time curves in furnace: (a) NSC columns, (b) HSC columns

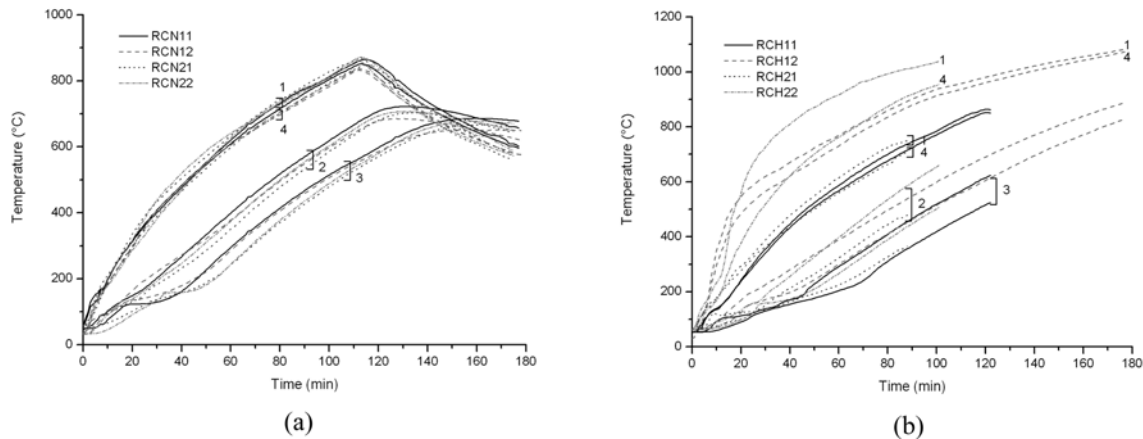


Fig. 9 Measured temperature-time curves at different locations: (a) NSC columns, (b) HSC columns

facing the gas burner during the fire test. Spalling on the side and its opposite side was observed after the test. Consequently the temperatures of these two points corresponding to RCH12 and RCH22 were markedly higher from 10-20 min after ignition (see Fig. 9).

Fig. 9 shows the recorded temperature profiles at four different locations (see Fig. 5) within the column mid-height section. Very similar results were obtained for all NSC specimens. Spalling of RCN22 did not seem to have an impact on the temperature developments. It might be due to the fact that the location of spalling had minor influence on the four thermocouples. The discrepancies among the experimental results were mainly caused by different heating curves and casting errors of thermocouples. Temperatures of the rebar (i.e., thermocouple 1 in Fig. 5) and the outer portion (thermocouple 4) of concrete decreased soon after the commencement of cooling phase. However, temperatures of the inner core part of concrete (thermocouple 2 and 3) continued to rise and exceeded those of the outer part during the later stage of cooling phase. The maximum temperatures of the bottom flange of the restraining beam and the surface of the enlarged cross section are around 30°C and 200°C, respectively, which indicated that the restraining beam and the column enlarged part were hardly influenced by increasing temperature.

4.3 Axial displacement at the top of columns

The structural model of the test assembly can be represented as shown in Fig. 10, where the linear spring represents the axial restraint of the whole restraining system. The stiffness of the spring was regarded as constant during the tests, because the maximum displacement at the center of the restraining beam was only about 13 mm. Thus, the restraining beam was taken as in the elastic range. Traditional test model considers a column as an isolated member resisting vertical load solely, in which case no axial restraint is considered and boundary conditions are regarded as pin-pin end or fix-fix end.

Fig. 11 shows a typical deformation-time curve for the specimens with axial restraint. The curve can be characterized by two different stages, i.e., expanding and contracting phases. The typical 'runaway' displacement failure of standard fire test on isolated columns is also shown in Fig. 11. The disparity between the two curves during the contracting phase can be attributed to the effect of axial restraint. In particular, the applied vertical load can be able to be gradually shifted to axial

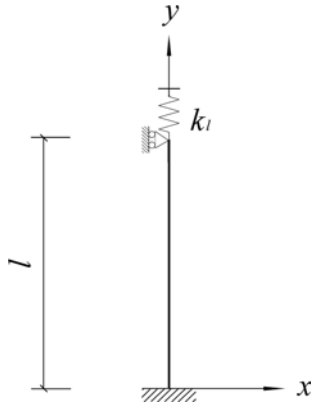


Fig. 10 Structural model of test assembly

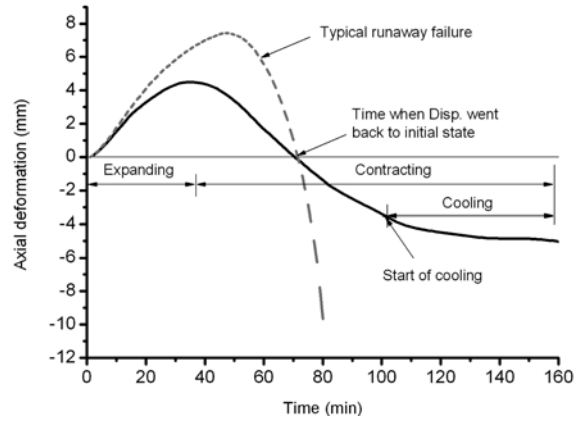


Fig. 11 Typical deformation-time curve

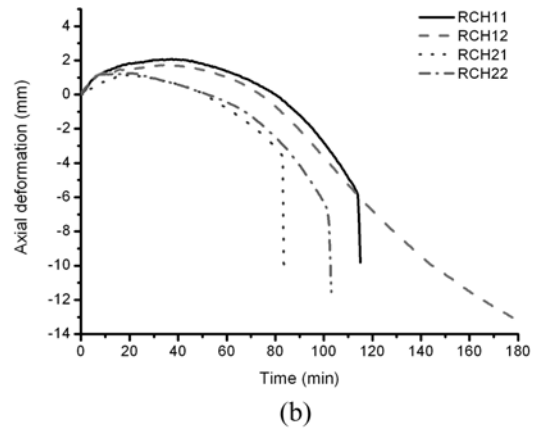
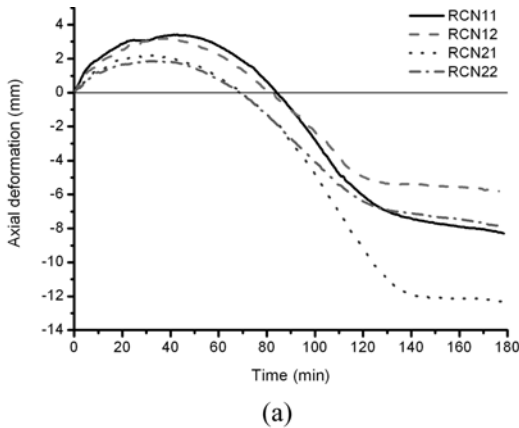


Fig. 12 Axial deformation-time relationships: (a) NSC columns, (b) HSC columns

restraint beyond the time when the column displacement goes back to the initial equilibrium state, whereas the applied load is constant and solely carried by the isolated column and a runaway failure would be observed.

Fig. 12 shows the recorded column axial deformation versus time relationships for all tests. The measured axial deformation was calculated from the readings of four evenly distributed LVDTs. It can be found in Fig. 12(a) that the deformations increased rapidly during the later stage of contracting phase of the two-hour heating. If it were not for the axial restraint provided by the restraining beam, the typical 'runaway' displacement would be observed and failure would be imminent. The rate of the deformation increase dropped quickly 5-10 minutes later after the fire went out. It is because that the inner parts of the concrete continued to rise (see thermocouple 2 and 3 in Fig. 9(a)). The deformation continued to increase slightly during the later cooling phase.

It can be seen in Fig. 12(a) that load ratio plays an important role on the fire behaviors of columns. The maximum deformations during expanding phase were influenced mostly by load ratio and hardly affected by axial restraint ratio. For a given load ratio, axial restraint ratio had a great influence on the development of axial deformation during contraction phase beyond the initial equilibrium state. We can also find that deformations of columns with the same axial restraint ratio

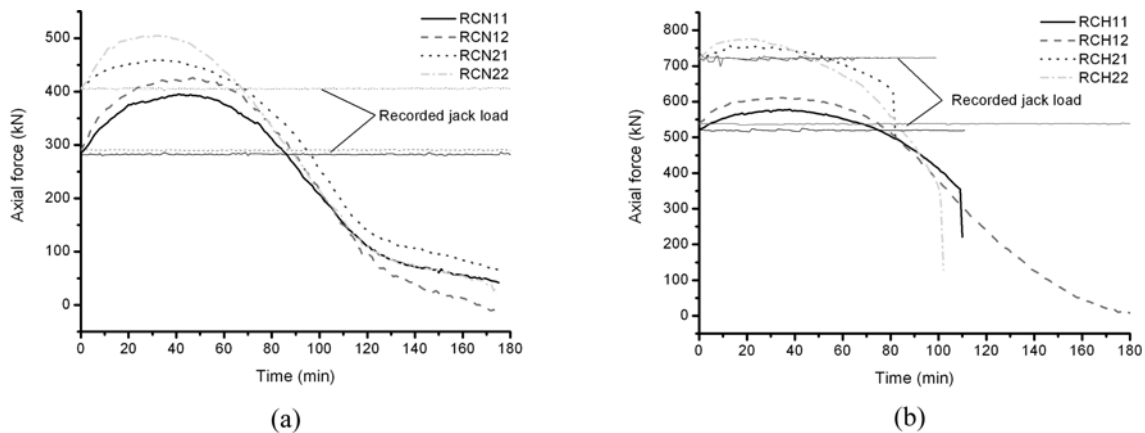


Fig. 13 Axial force-time relationships: (a) NSC columns, (b) HSC columns

followed very similar (nearly parallel) contraction path and all four columns experienced similar tendency during cooling phase. It can be noted that for columns with the same load ratio, the column deformations went back to zero at nearly the same time, regardless of the axial restraint ratios.

As for HSC columns, as can be seen in Fig. 12(b), there was an abrupt displacement drop during the contracting phase for test specimens RCH11, RCH21 and RCH22. Meanwhile, a corresponding sudden fall of axial force in the three columns was also recorded (see Fig. 13(b)). Both phenomena indicated that the columns could not endure the vertical load even with the help of the restraining beam. At this moment, the fire was stopped and the applied load was withdrawn in order to protect the testing facilities. The after-test inspection showed that there the concrete was crushed at nearly the mid-height of the three columns (see Figs. 7(e), (g) and (h)), explaining the unexpected descent of axial deformation. For test specimen RCH12, however, it managed to sustain the load with the aid of axial restraint without failure for a three-hour heating. This could be attributed to that, the column carried relatively less external load (same as RCH11) and at the same time received comparatively more axial restraint (same as RCH22) from the restraining beam. Both conditions were critical since without either one the column would have failed in the heating process.

4.4 Axial force in the restrained columns

In each test, the applied load was imposed before connecting the restraining beam to the reaction frame and kept constant during the fire exposure. Any additional load was taken by the restraining beam. After obtaining the internal forces of the axial spring (i.e., the restraining beam) according to the measured strains, the internal axial force in the restrained column can be found through force balance equation. Fig. 13 shows the variations of the internal axial forces for all the test specimens. The fluctuations of the applied loads during the tests, which were fairly small and within 5% of the designated loads, are also shown in Fig. 13.

As we can see in Fig. 13, for columns subjected to the same load ratio, the larger the axial restraint ratio is, the larger the maximum induced force and the less the axial force during the cooling phase are. The axial restraint ratio seems to have little effect on the development of column axial force during the contracting phase as well as cooling phase for columns under the same load

ratio. For the specimens without failure during the test, almost all the jack load was transferred to the restraining beam at the end of the test. The restraining beam took nearly all the vertical load.

We can see that the maximum induced forces in NSC columns are larger than those in the corresponding HSC columns. It is because NSC columns that exhibited larger maximum deformations during the expanding phase (see Figs. 12(a) and (b)). At the same time, NSC columns received relatively greater axial restraint for their comparatively lower column stiffness. None of the eight columns failed during the expanding phase because of the additional forces generated by the axial restraint. This is contradictory to the general assumption in the literature (Ali *et al.* 1998) that axial restraint would be an adverse effect on a heated column for it may accelerate the failure. We can notice in Fig. 13(a) that the axial restraint may help NSC columns to carry part of the load and prevent them from 'runaway' failure. The beneficial effect can be more directly perceived for HSC specimens in Fig. 13(b), where columns under the same load ratio, the one with a larger stiffness of axial restraint would have a better fire resistance. For example, the fire resistances of RCH21 and RCH22 are 82 min and 101 min, respectively.

Table 3 summarizes the experimental results. The time when the column is no more able to support the load which it supported before the fire, i.e., the time when the column axial displacement goes back to the initial value before fire started, is only relevant to the load ratio. For example, the time for RCN21 and RCN22 is around 70 min. But the load supported by a column in a structure before fire is usually far under its ultimate load bearing capacity. Therefore, the column can obviously undergo further contraction beyond that time as far as time goes-if the spring can manage to accommodate the shifted load from the column. However, it is not the case for RCH11, RCH21 and RCH 22. Even though the vertical load can be gradually transferred to the restraining beam, the columns had a sudden failure. It can be seen that when high-strength concrete was used, the behaviour of the RC columns changed. This may be due to the brittle nature of high-strength concrete. In a structure, it could be a local failure provided the rest of the structure can manage to sustain the released load. The load ratio and axial restraint ratio could certainly have an influence. For instance, RCH12 sustained the load with the help of the restraining beam under a three-hour heating.

It has to be noted that the restraining beam was placed outside of the furnace and remained unheated and undamaged during the tests. This is similar to the literature (Ali *et al.* 1998, Huang *et al.* 2007, Rodrigues *et al.* 2000, Tan *et al.* 2007) in which the stiffness of the restraint was

Table 3 Summary of experimental results

Type of concrete	Column No.	α	β	Time when axial disp. or force went back to initial state (min)		Fire resistance (min)
				Disp.	Force	
NSC	RCN11	0.24	0.0513	85	87	-
	RCN12	0.25	0.0772	81	90	-
	RCN21	0.35	0.0513	69	70	-
	RCN22	0.35	0.0772	70	71	-
HSC	RCH11	0.24	0.0445	80	75	119
	RCH12	0.25	0.0670	74	75	-
	RCH21	0.33	0.0445	52	56	82
	RCH22	0.34	0.0670	51	46	101

considered unchanged during the fire test. In reality, however, when a structure is in fire, beams may as well be exposed to fire. The strength and stiffness of beams could be weakened during heating because of exposure to high temperature and concrete cracking. Because of the limitation of the test equipment, the effect of varying stiffness of restraining beam was not considered. It can be achieved by numerical analysis, which is not the subject of the current paper and will be presented in a further study.

5. Conclusions

When a column is exposed to fire in a structure, it is restrained by surrounding structural members such as beams and slabs. When the column is subjected to fire, the load supported by the column can be transferred to the restraint if the structure can provide another load path. The following conclusions can be drawn based on the test results:

1. Axial restraint has an adverse effect on concrete spalling. The greater axial restraint a specimen received, the higher tendency concrete spalling would take place.
2. Increasing the axial restraint increased the value of restraint force generated in both the NSC and HSC columns. However, none of the columns failed due to additional forces induced by axial restraint during the expanding phase. It is contradictory to the general belief that axial restraint would yield an adverse effect on a heated column.
3. None of the four NSC columns failed during the contracting phase. Axial restraint helped the columns carry part of the vertical load in the contracting phase and prevented the column from 'runaway' failure. No deformation and strength reversal were observed during cooling for NSC columns. However, three of the HSC columns had a sudden axial displacement and force drop even with the help of axial restraint. It could be a local failure in the columns even if the structure can provide alternative load path. Increasing the axial restraint increased the failure time for HSC columns, however, it should be noted that this trend only obtained from several specimens in this paper, further studies are needed to verify this result.
4. The maximum deformations during expanding phase were influenced mostly by load ratio and hardly affected by axial restraint ratio. For a given load ratio, axial restraint ratio had a great influence on the development of axial deformation during contraction phase beyond the initial equilibrium state. The development of column axial force during the contracting phase followed nearly parallel trend for columns under the same load ratio.
5. Further investigation is needed concerning the deterioration of stiffness of the axial restraint when subjected to fire as well.

Acknowledgements

The research project was financially supported by National Natural Science Foundation of China (No.50738005, 50478078), the Ministry of Science and Technology of China (No.2006BAJ03A03-12), the Ministry of Education of China (No.NCET-04-0819) and the State Key Laboratory of Subtropical Building Science (2008ZA10). The authors are also grateful to Dr. Zhan-Fei Huang for his discussions and suggestions on the initial design of the restraining system.

References

- Ali, F. and O'Connor, D. (2001), "Structural performance of rotationally restrained steel columns in fire", *Fire Safety J.*, **36**(7), 679-691.
- Ali, F., Nadjai, A., Silcock, G. and Abu-Tair, A. (2004), "Outcomes of a major research on fire resistance of concrete columns", *Fire Safety J.*, **39**(6), 433-445.
- Ali, F.A., Shepherd, P., Randall, M., Simms, I.W., O'Connor, D.J. and Burgess, I. (1998), "The effect of axial restraint on the fire resistance of steel columns", *J. Constr. Steel Res.*, **46**(1-3), 305-306.
- Benmarce, A. and Guenfoud, M. (2005), "Behaviour of axially restrained high strength concrete columns under fire", *Construction and Building Materials*, V. In Press, Corrected Proof, No. pp. 476.
- Cabrita Neves, I. (1995), "The critical temperature of steel columns with restrained thermal elongation", *Fire Safety J.*, **24**(3), 211-227.
- Cabrita Neves, I., Valente, J.C. and Correia Rodrigues, J.P. (2002), "Thermal restraint and fire resistance of columns", *Fire Safety J.*, **37**(8), 753-771.
- Eurocode2 (2004), *European Committee for Standardization (Cen), Design of Concrete Structures: Part 1.2. General Rules – Structural Fire Design. Bs En 1992-1-2.*, Brussels (United Kingdom).
- Huang, Z.F. and Tan, K.H. (2004), "Effects of external bending moments and heating schemes on the responses of thermally restrained steel columns", *Eng. Struct.*, **26**(6), 769-780.
- Huang, Z.F., Tan, K.H. and Phng, G.H. (2007), "Axial restraint effects on the fire resistance of composite columns encasing I-section steel", *J. Constr. Steel Res.*, **63**(4), 437-447.
- Huang, Z.F., Tan, K.H. and Ting, S.K. (2006), "Heating rate and boundary restraint effects on fire resistance of steel columns with creep", *Eng. Struct.*, **28**(6), 805-817.
- Rodrigues, J.P.C., Cabrita Neves, I. and Valente, J.C. (2000), "Experimental research on the critical temperature of compressed steel elements with restrained thermal elongation", *Fire Safety J.*, **35**(2), 77-98.
- Tan, K.H., Toh, W.S., Huang, Z.F. and Phng, G.H. (2007), "Structural responses of restrained steel columns at elevated temperatures. Part 1: Experiments", *Eng. Struct.*, **29**(8), 1641-1652.
- Valente, J.C. and Neves, I.C. (1999), "Fire resistance of steel columns with elastically restrained axial elongation and bending", *J. Constr. Steel Res.*, **52**(3), 319-331.
- Wang, Y.C. (1997), "Effects of structural continuity on fire resistant design of steel columns in non-sway multi-storey frames", *Fire Safety J.*, **28**(2), 101-116.
- Wang, Y.C. (1999), "The effects of structural continuity on the fire resistance of concrete filled columns in non-sway frames", *J. Constr. Steel Res.*, **50**(2), 177-197.
- Wang, Y.C. and Davies, J.M. (2003a), "An experimental study of non-sway loaded and rotationally restrained steel column assemblies under fire conditions: analysis of test results and design calculations", *J. Constr. Steel Res.*, **59**(3), 291-313.
- Wang, Y.C. and Davies, J.M. (2003b), "An experimental study of the fire performance of non-sway loaded concrete-filled steel tubular column assemblies with extended end plate connections", *J. Constr. Steel Res.*, **59**(7), 819-838.
- Wang, Y.C. and Davies, J.M. (2003c), "Fire tests of non-sway loaded and rotationally restrained steel column assemblies", *J. Constr. Steel Res.*, **59**(3), 359-383.